Supporting Information

High Selectivity of an α-Conotoxin LvIA Analog for $\alpha3\beta2$ Nicotinic Acetylcholine Receptors is Mediated by $\beta2$ Functionally Important Residues

Xiaopeng Zhu,[1,2#] Si Pan,[3#] Manyu Xu,[3] Lu Zhang,[2] Jinfang Yu,[3] Jinpeng Yu,[1] Yong Wu,[1] Yingxu Fan,[4] Haonan Li,[2] Igor E. Kasheverov,[5,6] Denis S. Kudryavtsev,[5] Victor I. Tsetlin,[5,7] Yi Xue,[4] Dongting Zhangsun,[1,2] Xinquan Wang[3] and Sulan Luo[1,2*]*

[1] Medical School, Guangxi University, Nanning, 530004, China

[2] Key Laboratory of Tropical Biological Resources of Ministry of Education, Key Laboratory for Marine Drugs of Haikou, School of Life and Pharmaceutical Sciences, Hainan University, Haikou 570228, China;

[3] The Ministry of Education Key Laboratory of Protein Science, School of Life Sciences, Beijing Advanced Innovation Center for Structural Biology, Collaborative Innovation Center for Biotherapy, Tsinghua University, Beijing 100084, China

[4] Tsinghua-Peking Joint Center for Life Sciences, School of Life Sciences, Tsinghua University, Beijing 100084, China.

[5] Shemyakin-Ovchinnikov Institute of Bioorganic Chemistry, Russian Academy of Sciences, Miklukho-Maklaya Street 16/10, Moscow 117997, Russia.

[6] Sechenov First Moscow State Medical University, Institute of Molecular Medicine, Trubetskaya Street 8, bld. 2, 119991 Moscow, Russia.

[7] PhysBio of MePhi, Kashirskoe Ave.31, 115409 Moscow, Russia

Table of contents

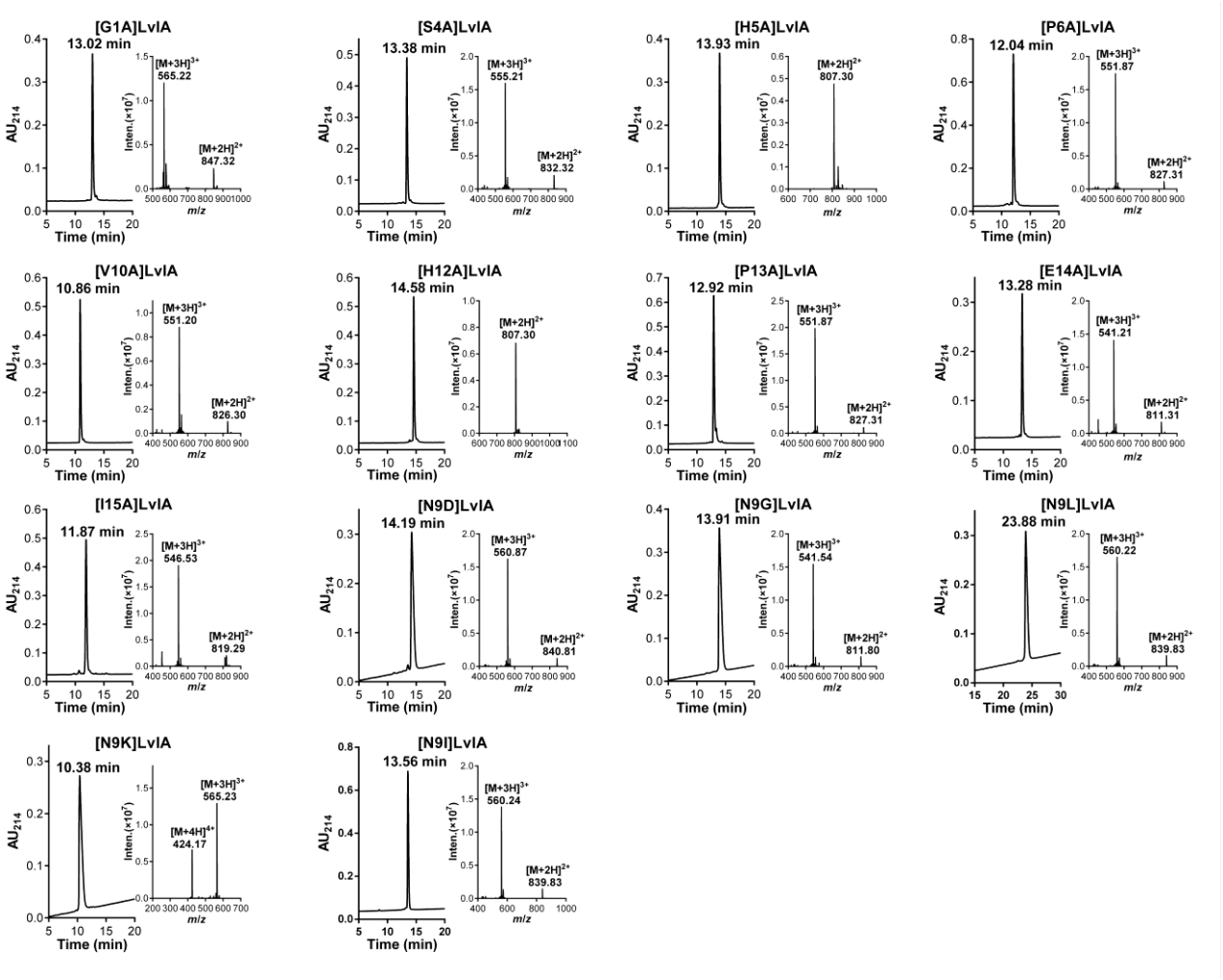

Figure S1. HPLC and Mass spectra profile of α-Conotoxin LvIA analogs. The LvIA analogs were analyzed on a reversed-phase analytical Vydac C18 HPLC using a linear gradient of 5% to 40% buffer (0.5% TFA and 90% acetonitrile) over 30 min. Absorbance was monitored at 214 nm. The molecular weight was determined by electrospray ionization mass spectrometry (ESI-MS)

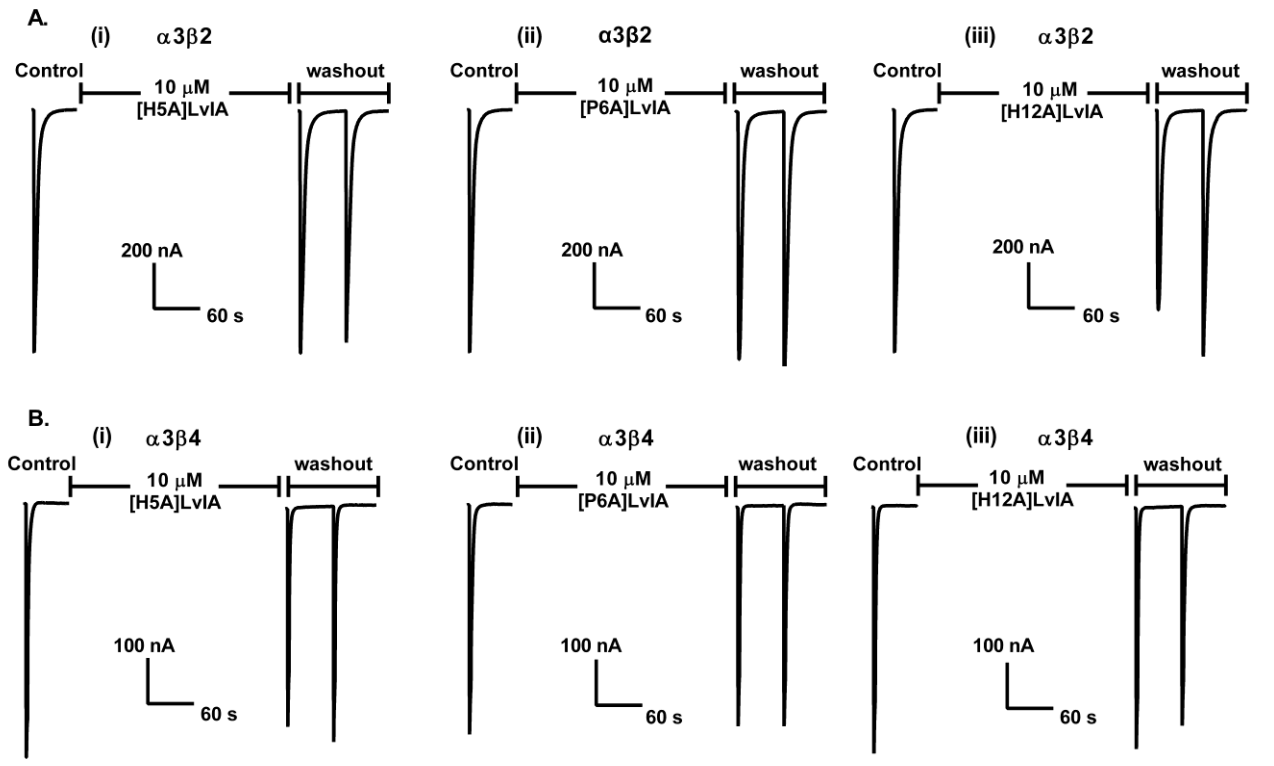

Figure S2. Three LvIA analogs have no potency at rat α3β2 and α3β4 nAChRs. *Xenopus* oocytes expressing α3β2 and α3β4 nAChRs were voltage clamp at -70 mV and subjected to a 2-s pulse of 100 μM ACh every minute as described under Experimental Section. In each series, the Control represents control response to ACh, following which the oocytes were exposed to 10 μM LvIA analogs for 5 min, respectively. The perfusion and ACh pulses were then resumed to measure the response to ACh during washout of LvIA and analogs. Inhibition of currents with [H5A]LvIA (i), [P6A]LvIA (ii) and [H12A]LvIA (iii) on the α3β2 (A) and α3β4 (B) nAChRs, respectively.

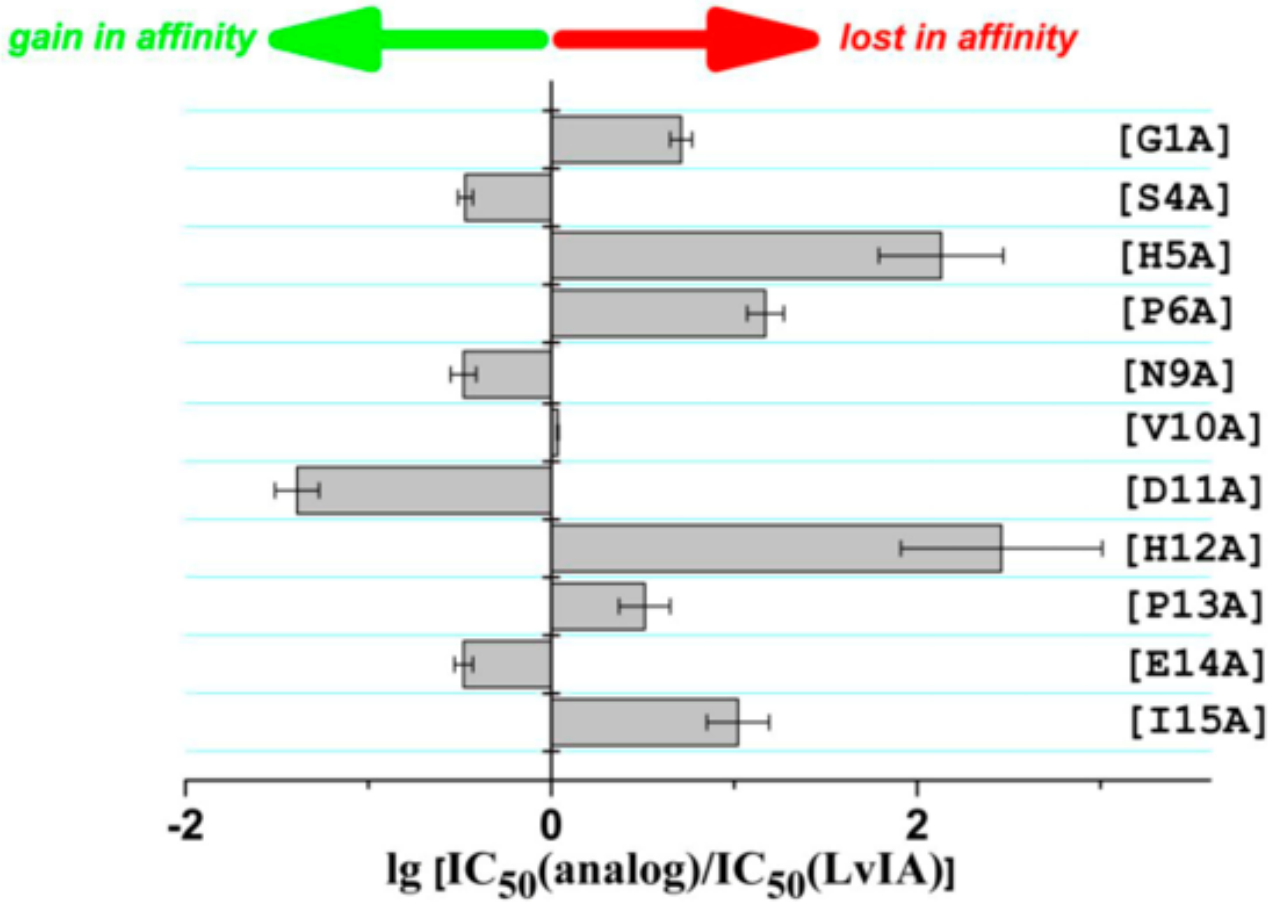

Figure S3. Bar presentation of the change in potency of each analog of α-Conotoxin LvIA for *Ac*-AChBP. This change was evaluated as logarithm of ratio of IC_{50} values for respective analog and LvIA. A decrease in affinity to *Ac*-AChBP for concrete analog as referred to LvIA is represented with bars below red arrow; and an increase—below green arrow.

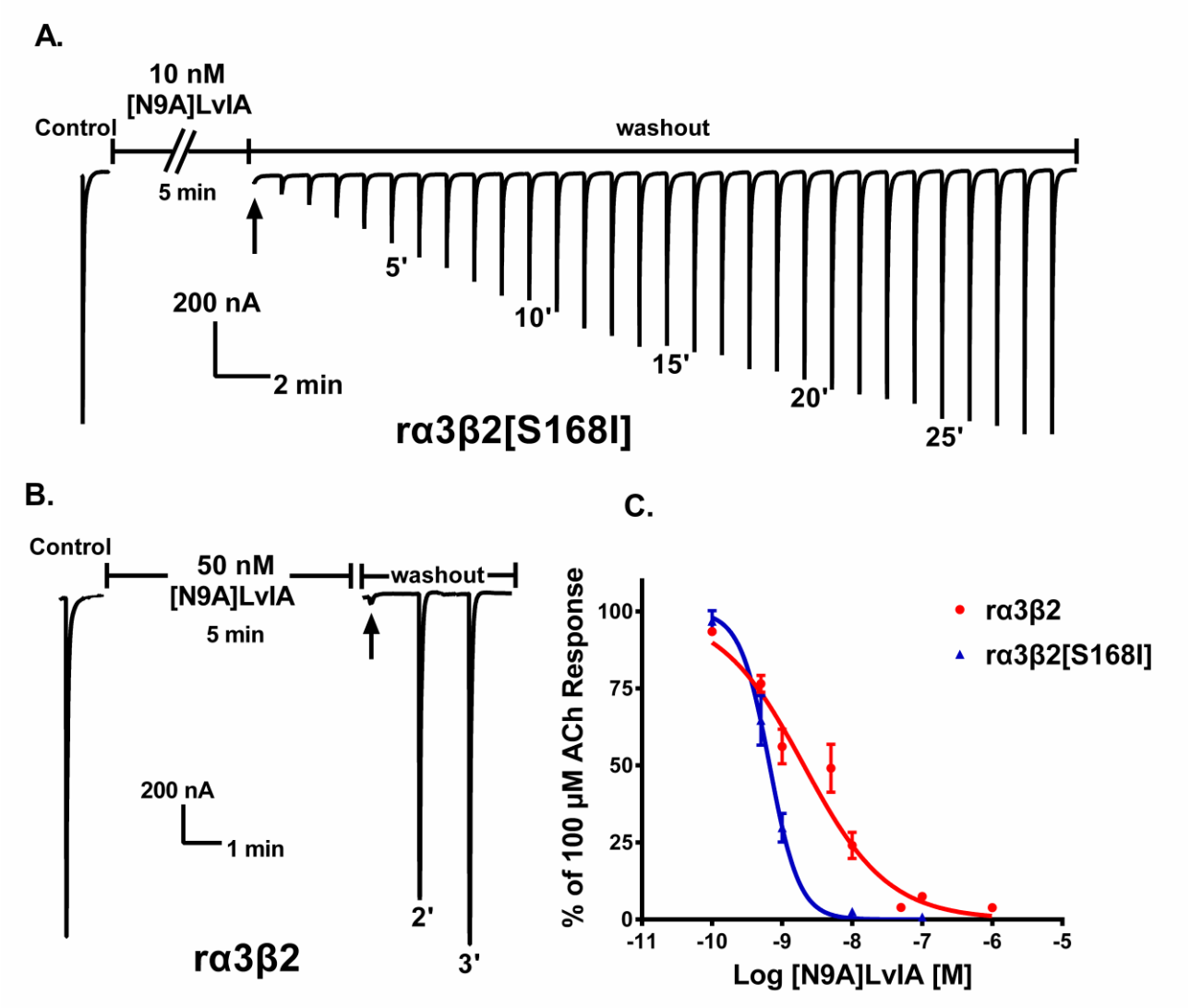

Figure S4. [N9A]LvIA blocks the rat α3β2[S168I] nAChR mutant. *Xenopus* oocytes expressing α3β2[S168I] nAChR mutant was voltage clamp at -70 mV and subjected to a 2-s pulse of 100 µM ACh every minute as described under Experimental Section. In each series, the Control represents control response to ACh, following which the oocytes were exposed to 10 nM [N9A]LvIA for 5 min. The perfusion and ACh pulses were then resumed to measure the response to ACh during washout of [N9A]LvIA. Inhibition of currents with [N9A]LvIA on the α3β2[S168I] mutant **A** and WT α3β2 **B**; **C** represents concentration-response analysis for inhibition of α3β2[S168I] nAChRs mutant by [N9A]LvIA .

Table S1. Contacting amino acid residues between α-CTx and Ac-AChBP with a distance cutoff 4.0 Å.

AChBP	[N9A]LvIA	[D11A]LvIA
	Principal side	
Tyr-91		His-5
Trp-145	Ala-7	Pro-6, Ala-7
Ser-148	Asp-11	
Glu-151	Asp-11	
Tyr-186	His-5	Gly-1, His-5
Ser-187		Gly-1
Cys-188	Cys-2	Cys-2
Cys-189	Cys-2, Cys-8, His-12	His-12
Glu-191	Asp-11, His-12	His-12
Tyr-193	Ala-7, Cys-8, Asp-11	Ala-7, Cys-8, His-12
	Complementary side	
Thr-34	Cys-3	Cys-3
Gln-55	Cys-3, Cys-16	Asn-9, Cys-16
Arg-57	Ala-9, Val-10, Pro-13	Pro-13-Cys-16
Asp-75	Asp-11	
Arg-77	Asp-11	
Met-114	Ala-9	Ala-9, Val-10
Asp-157	Cys-16	Cys-16
Asp-162	Cys-3, Ser-4	Cys-3, Ser-4
Ser-164	Gly-1, Ser-4	Gly-1, Ser-4
Ser-165	Ser-4, His-5	Ser-4

Table S2. Modeled contacts of α-CTxs [N9A]LvIA and [D11A]LvIA with rα3β2 and rα3β4, respectively.

[N9A]LvIA-rα3β2 model		[N9A]LvIA-rα3β4 model		[D11A]LvIA-rα3β2 model		[D11A]LvIA-rα3β4 model	
rα3β2	**[N9A]LvIA**	**rα3β4**	**[N9A]LvIA**	**rα3β2**	**[D11A]LvIA**	**rα3β4**	**[D11A]LvIA**
			Principal side				
Trp-150	Ala-7	Trp-150	Ala-7	Tyr-94	His--5	Tyr-94	His-5
Asp-153	Asp-11	Asp-153	Asp-11	Trp-150	Ala-7	Trp-150	Ala-7
Tyr-191	His-5	Tyr-191	His-5	Tyr-191	His-5	Tyr-191	Gly-1, His-5
Glu-196	His-12	Glu-196	His-12	Glu-196	His-12	Glu-196	His-12
Tyr-198	Ala-7, Asp-11, His-12	Tyr-198	Asp-11, His-12	Tyr-198	His-12	Tyr-198	His-12
			Complementary side				
Lys-79	Asp-11	Lys-59	Cys-16	Lys-79	Ala-11	Lys-59	Asn-9, Cys-16
Arg-81	Asp-11	Arg-81	Asp-11	Lys-163	Pro-13, Cys-16	Arg-113	Val-10, Ala-11
Val-111	Val-10	Arg-113	Val-10, Asp-11	Asp-170	Gly-1	Gln-119	Val-10, Pro-13
Phe-119	Ala-9	Gln-119	Val-10	Asp-171	Ser-4	Lys-163	Cys-16
Lys-163	Pro-13, Cys-16	Lys-163	Pro-13, Ile-15			Asp-170	Gly-1
Ser-168	Gly-1, Ser-4	Asp-170	Gly-1				
Asp-170	Gly-1	Asp-171	Ser-4, His-5				
Asp-171	His-5						

Table S3. Sequences of primers used to construct point mutants

No.	Mutant	Primer (5'-3')
1	β2(F106V)	FM: GCATGTACGAAGTCTCCGTCTATTCCAATGCTGTG RM: CACAGCATTGGAATAGACGGAGACTTCGTACATGC
2	β2(S108T)	FM: CATGTACGAAGTCTCCTTCTATACGAATGCTGTGGTCTCCTATGATG RM: CATCATAGGAGACCACAGCATTCGTATAGAAGGAGACTTCGTACATG
3	β2(A110V)	FM: GTCTCCTTCTATTCCAATGTTGTGGTCTCCTATGATGGC RM: GCCATCATAGGAGACCACAACATTGGAATAGAAGGAGAC
4	β2(S113R)	FM: CAATGCTGTGGTCCGCTATGATGGCAGC RM: GCTGCCATCATAGCGGACCACAGCATTG
5	β2(Y114S)	FM: CCAATGCTGTGGTCTCCTCTGATGGCAGCATCTTTTG RM: CAAAAGATGCTGCCATCAGAGGAGACCACAGCATTGG
6	β2(D115N)	FM: CAATGCTGTGGTCTCCTATAACGGCAGCATCTTTTGGCTAC RM: GTAGCCAAAAGATGCTGCCGTTATAGGAGACCACAGCATTG
7	β2(D165P)	FM: GGTGCTCAAAAGTCCTGTGGCCAGTCTG RM: CAGACTGGCCACAGGACTTTTGAGCACC
8	β2(V166T)	FM: GGTGCTCAAAAGTGATACGGCCAGTCTGGATGAC RM: GTCATCCAGACTGGCCGTATCACTTTTGAGCACC
9	β2(S168I)	FM: CTCAAAAGTGATGTGGCCATTCTGGATGACTTCACACCC RM: GGGTGTGAAGTCATCCAGAATGGCCACATCACTTTTGAG
10	β2(L169M)	FM: CAAAAGTGATGTGGCCAGTATGGATGACTTCACACCCA RM: CTGGGTGTGAAGTCATCCATACTGGCCACATCACTTTTG

Table S4. Data collection and refinement statistics

Data collection	**Ac-AChBP/LvIA[N9A]**	**Ac-AChBP/LvIA[D11A]**
Beamline	SSRF BL17U	TPS 05A
Wavelength	0.9796 Å	2.26-0.62 Å
Space group	*P* 4_1 2_1 *2*	*P 65*
Cell dimensions		
a, b, c (Å)	207.441, 207.441, 114.061	173.08, 173.08, 118.337
α, β, γ (°)	90, 90, 90	90, 90, 120
Resolution (Å)	50.00-3.00	50.00-2.89
[a]R_{merge}	0.265 (1.752)	0.081(0.759)
[b]R_{pim}	0.079 (0.504)	0.048(0.447)
[c]$CC_{1/2}$ of the highest resolution shell	0.987 (0.747)	0.640
I/δI	9.376 (1.612)	15.817(1.824)
Completeness (%)	99.99 (100)	98.8(100)
Redundancy	13.2	3.7
Refinement		
Resolution (Å)	46.39-2.998 (3.105-2.998)	39.22-2.803(2.903-2.803)
No. reflections	48357(4859)	49433(4901)
[d]R_{work}/R_{free} (%)	0.2635/0.3189	0.2045/0.2681
No. atoms	8820	8818
macromolecules	8815	8813
ligands	5	5
Wilson B-factor ($Å^2$)	56.07	84.58
Average B-factors ($Å^2$)	59.84	83.05
macromolecules	59.83	83.04
ligands	80.77	100.79
r.m.s. deviations		
Bond lengths (Å)	0.013	0.012
Bond angles (°)	1.54	1.32
Ramachandran plot (%)		
Favored	97	92
Allowed	3	7.2
Outlier	0.091	0.55

NOTE. [a]$R_{merge} = \sum_{hkl} \sum_j |I_j(hkl)-\langle I(hkl)\rangle| / \sum_{hkl} \sum_j I_j(hkl)$, where *I* is the intensity of reflection.

[b]$R_{pim}=\sum_{hkl} [1/(N-1)]^{1/2}\sum_j |I_j(hkl)-\langle I(hkl)\rangle| / \sum_{hkl} \sum_j I_j(hkl)$, where *N* is the redundancy of the dataset.

[c]$CC_{1/2}$ is the correlation coefficient of the half datasets.

[d]$R_{work} = \sum_{hkl} | |F_{obs}| - |F_{calc}| | / \sum_{hkl} |F_{obs}|$, where F_{obs} and F_{calc} is the observed and the calculated structure factor, respectively. R_{free} is the cross-validation *R* factor for the test set of reflections (5% of the total) omitted in model refinement.